PERGAMON

Journal of Geodynamics 32 (2001) 311–332

JOURNAL OF GEODYNAMICS

www.elsevier.com/locate/jgeodyn

Strain-dependent stress field and plate motions in the south-east Aegean region

Sotirios Kokkalas, Theodor Doutsos*

Department of Geology, University of Patras 26 500 Patras, Greece

Received 22 May 2001; accepted 18 June 2001

Abstract

In the south-eastern Aegean region, we record stress and strain established in two stages, during the convergence of the African with the Eurasian plate: the late collision of the Hellenides and the fore-arc evolution above the Hellenic subduction. Observed directions of principal stress axes associated with these stages are not in good correlation with the motion direction of the converging plates and are strongly depended to a pre-existed orthogonal fault system, which comprises WNW–ESE and NNE–SSW trending faults. At present, imposition of shear stress along the south-eastern margin of the Aegean plate causes a great variation of stress, while re-activated NNE-SSW trending faults transfer the plate motion of Anatolia south-westwards to the Hellenic Trench.

1. Introduction

Large areas in the interior of continents have stress orientations that are constant and parallel to the absolute plate motions (Zoback, 1992). However, smaller-scale deviations from this 'far-field stress' are often observed and termed as 'regional-or local stress field' in close correspondence with the second and third order stress field (sensu Zoback, 1989). This stress variability is reported from plate margins (Rebai et al., 1992; Andeweg et al., 1999; Hillis and Reynolds, 2000) as well as from smaller areas with an inherited structural grain, faults etc. (Mattauer and Mercier, 1980; Sassi and Faure, 1997). Additional variability is caused by displacements along crustal anisotropies (Tikoff and Wojtal, 1999) and make difficult to correlate between stress field and plate motions.

* Corresponding author. Tel.: +30-61-997841; fax: +30-61-994485.
E-mail addresses: tdoutsos@upatras.gr (T. Doutsos), skokalas@upatras.gr (S. Kokkalas).

0264-3707/01/$ - see front matter
PII: S0264-3707(01)00035-7

The south Aegean region with a large temporal and spatial stress variation (Angelier et al., 1982; Mercier et al., 1989; Doutsos and Kokkalas, 2001) and the great number of studies regarding the motion vectors of the African and Aegean plates (Dewey et al., 1989; Billiris et al., 1991; Le Pichon et al., 1995; Kahle et al., 1998) offers an opportunity to make such a correlation. We chose to study the southeastern Aegean region for two reasons: (1) It posesses a fore-arc position near the Pliny and Strabo trench segments of the Hellenic Arc which act as transcurrent faults (Mc Kenzie, 1978; Huchon et al., 1982) and (2) there are pre-existing faults obliquely oriented to the main structural grain of the area (Kokkalas and Doutsos, 2000). We analyse stress distribution in the area and emphasise the role of pre-existing faults to produce local stress fields as well as to transfer large scale block movements.

2. Tectonic setting

2.1. Collision

The Hellenides is an arcuate fold and thrust belt which is connected to the Dinarides to the north and to the Taurides to the southeast (Fig.1, inset). They are the result of collision between the Eurasian continent and the Apulian plate (Dewey et al., 1973). The latter is interpreted as a large microcontinent or a promontory of Gondwana to the south (see Robertson et al., 1991). Rifting during Triassic and Jurassic times divided this microcontinent into several palaeogeographic terranes, which included a shallow platform at the centre (Tripolitsa zone) and deep basins to the southwest (Ionian zone, Plattenkalk series) and to the northeast (Pindos zone, see Bernoulli and Laubscher, 1972; Jacobshagen et al., 1978). The Apulian microcontinent is bounded to the east by an ophiolitic suture zone, the ''Pindos suture'', which extends from the Dinarides through Peloponnesus to the Cretan sea (Fig. 1; Smith, 1977). Crustal wedging occurring along this suture, at the Oligocene-early Miocene, resulted in the formation of the large nappe systems of southwest Hellenides and the tectonic windows of Peloponnesus and Crete (Stockhert et al., 1995; Doutsos et al., 2000; Xypolias and Doutsos, 2000).

A well known tectonostratigraphic column in the southeastern Hellenides is reported from central and eastern Crete (Fig. 2; Creutzburg and Seidel, 1975; Fassoulas et al., 1994), whereas for the Dodecanese islands further east only stratigraphic correlations are available (Blondeau et al., 1975; Aubouin et al., 1976). In Crete, the tectonic windows contain a rim of non-metamorphic nappes (Pindos and Tripolitsa nappes) and a core of HP/LT metamorphic nappes (PQ and PLK series, Fig. 2). The last underwent a HP/LT metamorphism with P–T conditions ranging between 300 and 400°C and 8–10 kbar (Seidel et al., 1982). These rocks must have been exhumed from $\sim$30 to $<$10 km before $\sim$19 Ma, at a minimum rate of $\sim$4 mm/year (Thomson et al., 1998). In the metamorphic nappes a well defined NNW–SSE trending stretching lineation indicates the transport direction of the nappes (Fig. 2; Kokkalas and Doutsos, 2000). Contractional movements lasted until the Middle Miocene, as it is indicated by late orogenic thrusts within the adjacent sedimentary basins (Postma et al., 1993; Boronkay and Doutsos, 1994; Ten Veen and Postma, 1999). However, stress field data and three dimensional deformation analysis of this late orogenic event in the southeast Hellenides are missing.

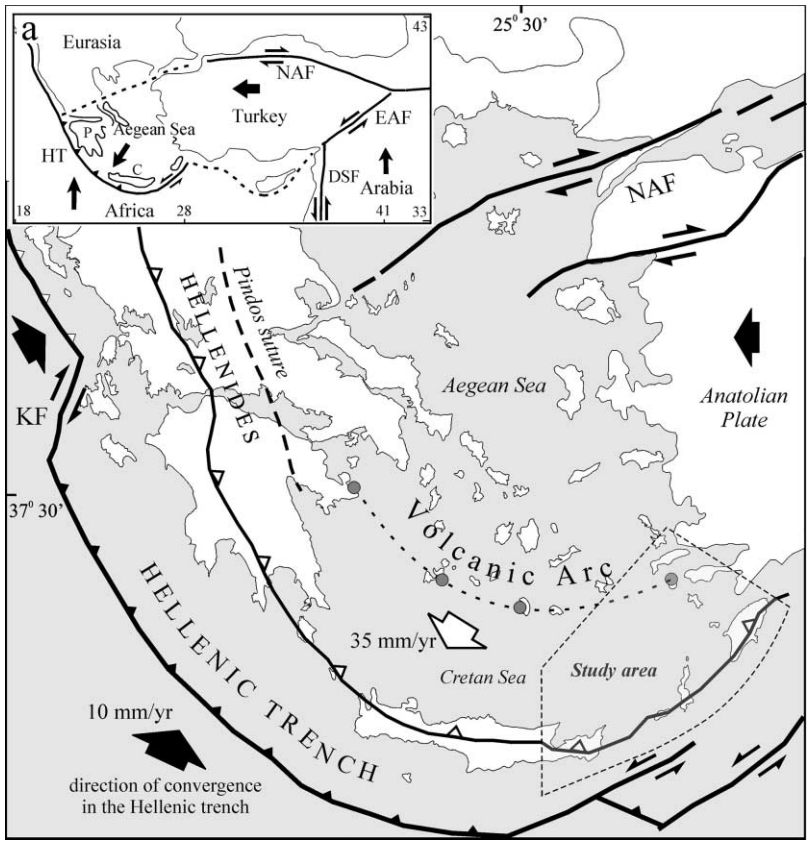

Fig. 1. (a) Simplified map showing the main structural features of the Hellenic Arc and Trench system. KF = Kefallonia Fault, NAF = North Anatolian Fault. Inset a: Schematic map summarizing the geodynamic framework in the eastern Mediterranean with the major plates involved in collision process (after McKenzie, 1972). NAF = North Anatolian Fault, EAF = East Anatolian Fault, DSF = Dead Sea Fault, HT = Hellenic Trench, P = Peloponnesus, C = Crete.

2.2. Stratigraphy and sedimentation

We provide here a summarized stratigraphic evolution of key basins because the stratigraphic analysis enabled the distinction of fault sets into subsets. Since Late Miocene, south Hellenides lay in a fore-arc position within the Hellenic Arc and underwent extension genetically related with two first-order structures: the North Anatolian transform fault (NAF) and the Hellenic subduction zone (McKenzie, 1972; Dewey and Sengor, 1979; Le Pichon and Angelier, 1979; Jackson, 1994). This extension is accommodated by a non-orthogonal system of WNW–ESE trending normal faults which caused by arc-normal pull acting on the Aegean plate and NE–SW trending transfer faults which have transfered some of the motion of the Anatolia block toward the southern Aegean area (Doutsos and Kokkalas, 2001).

Le Pichon and Angelier (1979) and Angelier et al. (1982) produced a reconstruction of the Aegean before the onset of the present-day extensional regime. This was based mainly on the length of the seismically active subducted slab in the Hellenic trench and bathymetry variations in

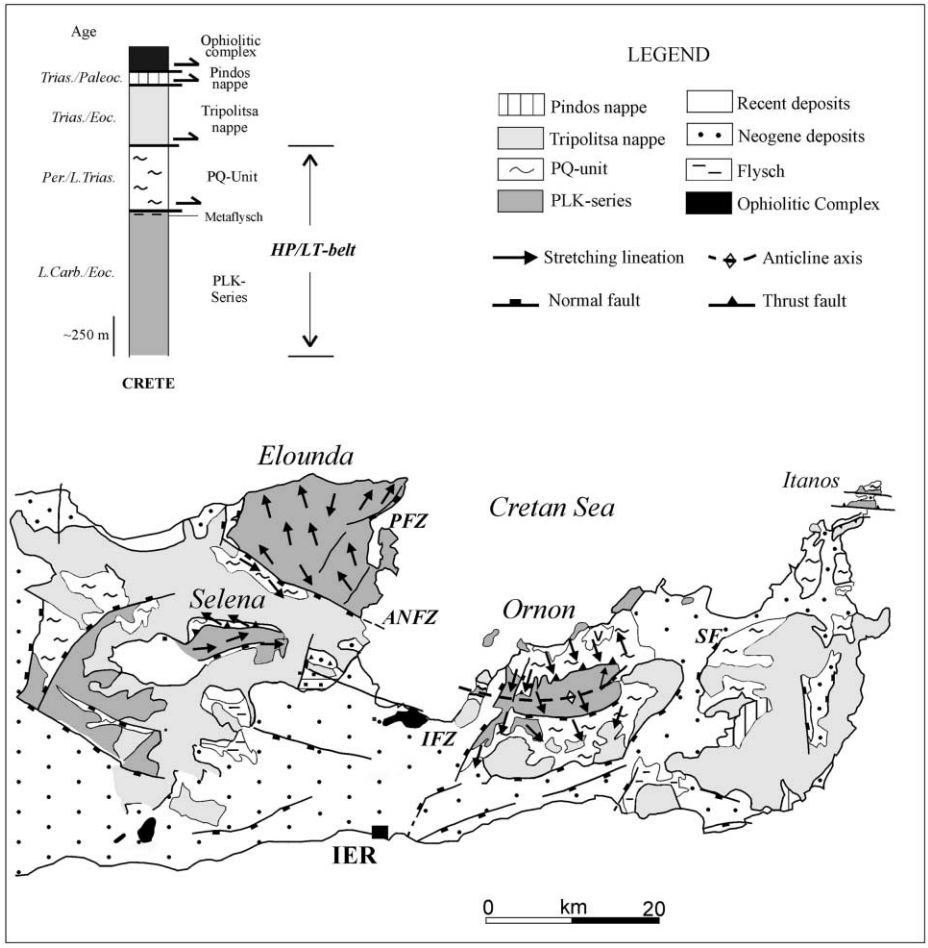

Fig. 2. Map of eastern Crete with tectonostratigraphic column and the main structural features.

the Aegean. Their reconstruction restores the convex bulge of the Aegean Arc to an essentially WNW–ESE trending linear feature. As suggested by palaeomagnetic studies clockwise rotations up to 45° occurred in the western segment of the arc since Middle Miocene times (Kissel and Laj, 1988), whereas counter-clockwise rotations up to 30° in the eastern segment began later in the Lower Pliocene (Duermeijer et al., 2000).

Fore-arc extension strongly modified the collisional structures leading to the break-up of the Aegean region since the Serravallian (Drooger and Meulenkamp, 1973). Offshore and onshore basins (Fig. 3) were filled with up to 1500 m thick sediments and Crete and the Dodecanese Islands were formed. In eastern Crete, sedimentation started with open marine Upper Miocene shelf, slope and basin-floor facies in the Ierapetra and Fothia basins and by mainly shelf-facies in the smaller basins of the Sitia region (Fig. 3a; Fortuin, 1977, 1978; Postma et al., 1993). The lowermost Pliocene sediments are generally found as slump components and debris-flow deposits (Fortuin, 1977). Deep marine marls and clays continued in the sedimentary succession. Finally,

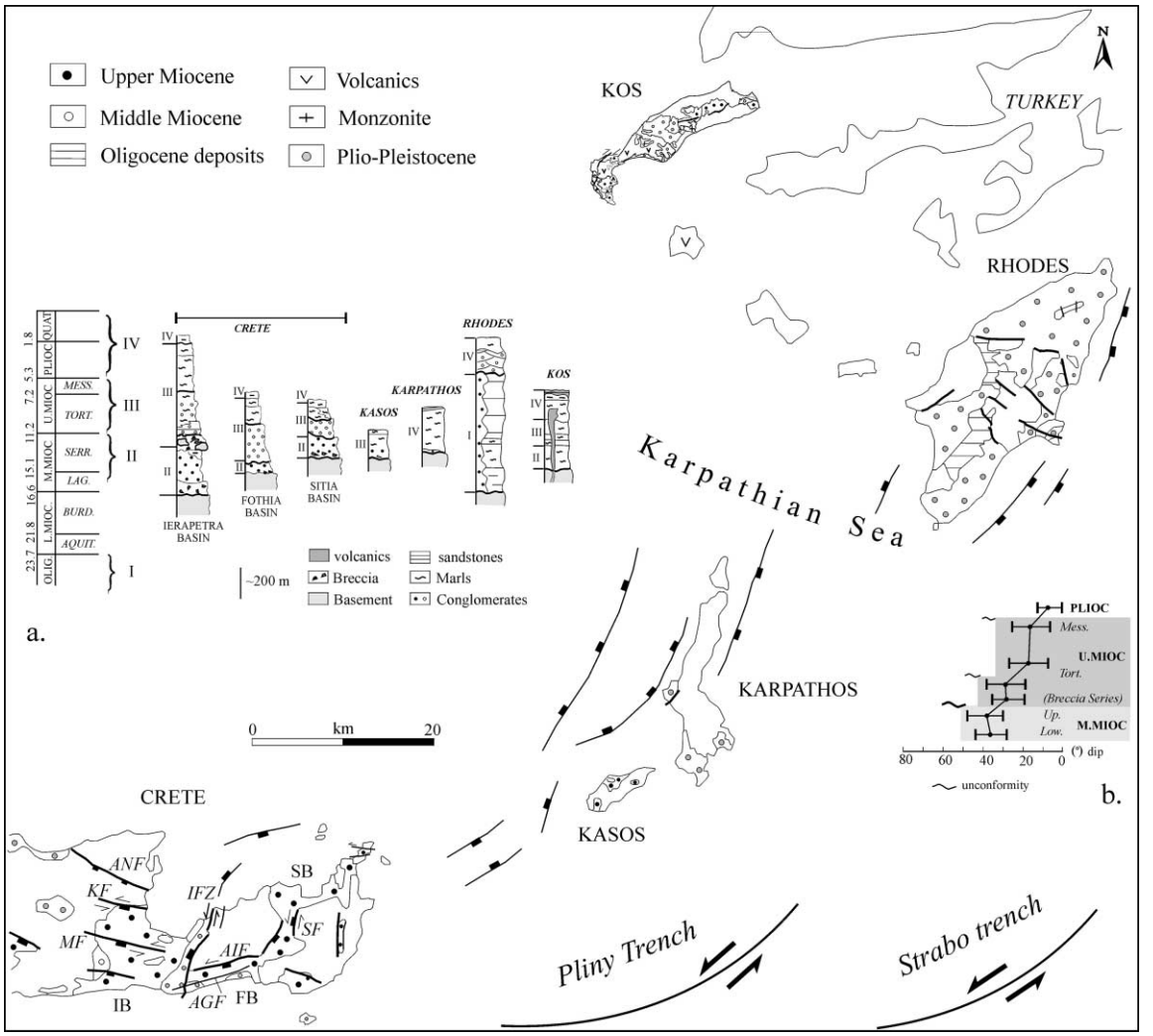

Fig. 3. Simplified map of SE-Aegean, showing the location of basins and (a) synthetic stratigraphic sections of the Neogene succession, for each island. (b) Dip data grouped by stratigraphic age showing regional variation in dip values and significant changes (unconformities). The diagram shows, the mean (dot) and the range of measurements (1 standard deviation). AGF = Ag. Fothia Fault, AIF = Ag. Ioannis Fault, ANF = Ag. Nikolaos Fault, KF: Kritsa Fault, MF: Makrilia Fault, IFZ: Ierapetra Fault zone, SF: Sitia Fault, IB: Ierapetra basin, SB: Sitia basin, FB: Fothia basin.

the Quaternary deposits comprise bioclastic limestones and Tyrrhenian marine terraces which are found mainly at the south coast of Ierapetra basin (Angelier and Gigout, 1974; Pirazzoli et al., 1982).

On Kasos Island, the basin fill comprises red conglomerates at the base and yellow marls at the upper parts of the succession. The age of the Neogene sediments, which lie uncomformably above the basement units, correlates with the lower part of Upper Messinian (Dermitzakis and Triantaphyllou, 1991). On Karpathos Island, marine marls of Pliocene age uncomformably overlie the

pre-Neogene folded basement rocks (Buttner and Kowalczyk, 1978). These are, in turn, overlain by fossiliferous calcarenites of late-Pliocene/Pleistocene age (Barrier et al., 1979), on which marine terraces of Tyrrhenian age were formed (Barrier and Angelier, 1982).

Further north on Rhodes Island, a middle-upper Oligocene succession (Vati-Group; Mutti, 1965) is exposed mainly in the southern part of the island. This succession consists of conglomerates and sandstones at the lower part followed by deep-water marls. Turbiditic sandstones with some conglomerates and slump sediments comprise the upper parts (Mutti, 1965; Mutti et al., 1970). These deposits uncomformably overlie a strongly folded lower Oligocene flysch. Sedimentation continued above an uncomformity with the deposition of thick Pliocene fluviatile and lacustrine deposits (Mutti et al., 1970; Meulenkamp et al., 1972) followed up by late-Pliocene-Pleistocene marine, clastic deposits as well as terrigenous pelagic muds and deep-water carbonates (Hanken et al., 1996).

Finally, on Kos Island the deposition of marine sediments of lower-middle Miocene age was followed by the accumulation of upper Miocene lacustrine sediments (Boger et al., 1974). At approximately 12 Ma, a large quartz monzonite intruded the basement units (Altherr et al., 1982; Henjes-Kunst et al., 1988). From the Middle Pliocene to Pleistocene a continuous sequence of continental to marine facies was deposited (Boger et al., 1974; Besenecker and Otte, 1978; Willmann, 1983). Volcanic activity on Kos Island first began in the Pliocene and early Pleistocene, when calc-alkaline dacitic and rhyolithic domes and rhyolithic phreatomagmatic deposits were erupted in the Kefalos Peninsula on western Kos (Bellon and Jarrige, 1979; Keller et al., 1990), producing both ash falls and ignimbrites. The eruption of the Kos Plateau Tuff, which consists of co-ignimbrite lithic breccias, occurred at approximately 160 ka (Smith et al., 1995).

3. Stress analysis

In order to analyse the stress field in the post-Oligocene sediments of the south-east Hellenides, we studied the brittle deformation in 36 different stations (Figs. 4, 6 and 7) The data consist of measurements of striation and sense of motion along a series of fault planes. The sense of slip on a fault surface is deduced using criteria summarised by Hancock (1985) and Petit (1987), i.e. arrays of en echelon cracks, kink bands, stylolithes, fibrous veins etc. The fault-slip data have been collected from basin-bounding faults, as well as from mesoscopic faults in the Middle Miocene to recent basins. We collected fault-slip data close to the centre of all the fault surfaces in order to constrain regionally significant tension directions and to avoid slip-vector variance, occurring along faults (Jackson et al., 1982; Roberts, 1996).

In order to establish a new stress map of the study area, we used different methods for the analysis of structural data. The graphical methods of stress analysis (P–T axes: Turner, 1953, right dihedron: see Angelier, 1994) were used for a first approximation of the stress axes, while the numerical methods (direct inversion: see Angelier, 1994; numerical dynamic analysis: Spang, 1972) helped in the accuracy of the results for the principal stress axes determination. The results obtained from the different methods correspond closely. Moreover, it should be noted that although some of the above mentioned methods (P–T axes method by Turner, 1953; numerical dynamic analysis by Spang, 1972) were introduced for stress analysis using deformation lamallae of calcite, in current geological literature these methods are also applicable in fault-slip analyses.

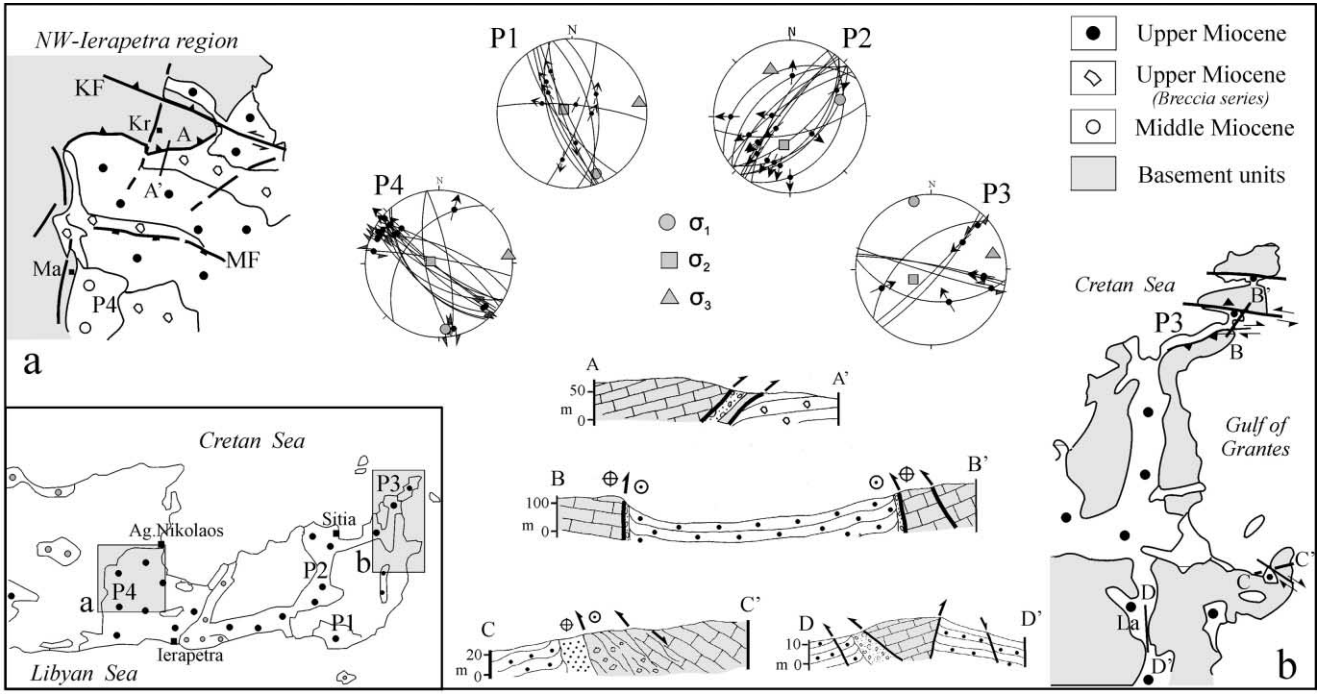

Fig. 4. Middle Miocene contractional structures in eastern Crete. Location of map-areas and stereonets are shown in inset. Site numbers on stereonets refer also to Table 1. KF = Kritsa Fault, MF = Makrilia Fault, Ma = Males village, Kr = Kroustas village, La = Lagada

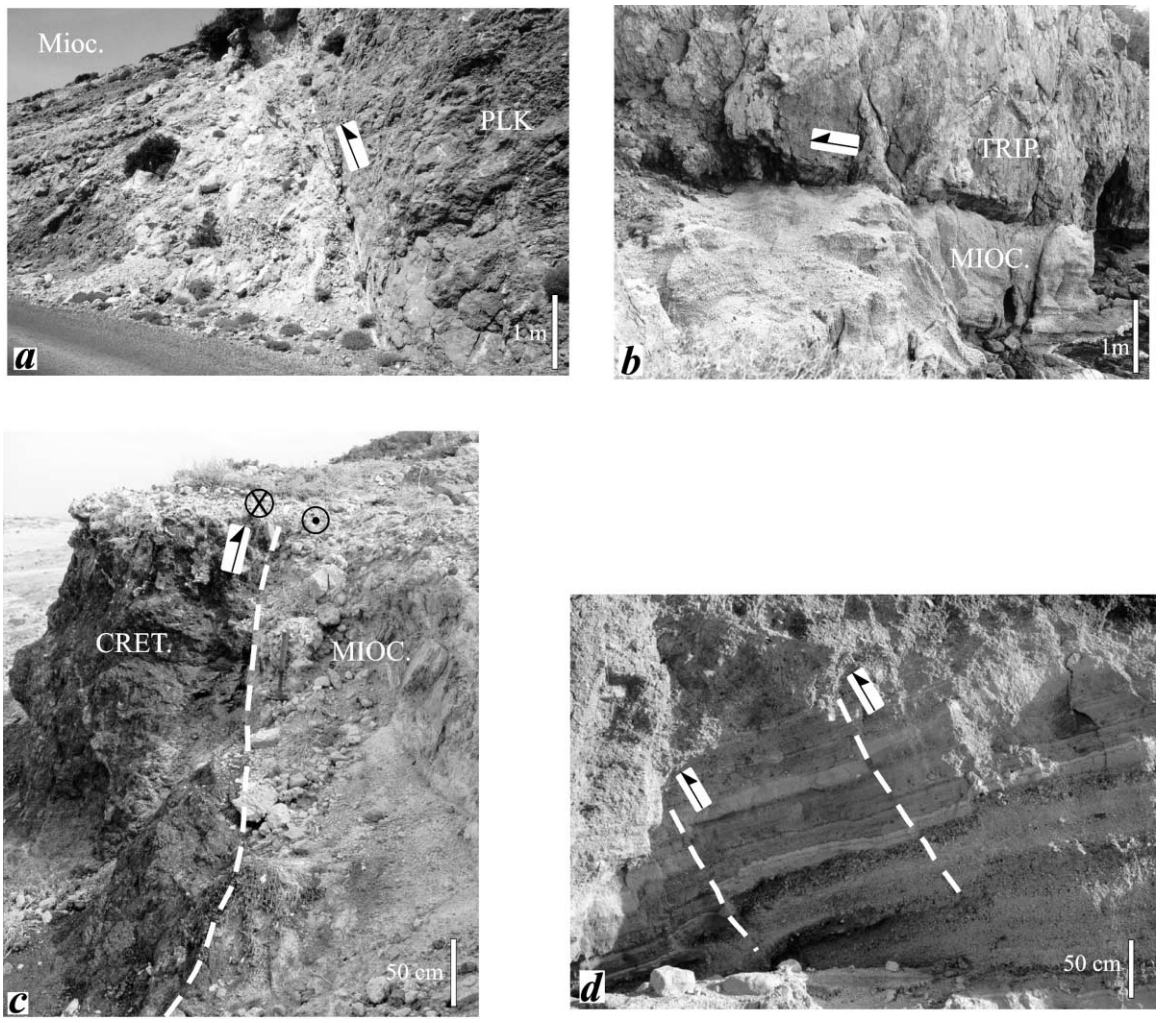

Fig. 5. (a) The northern, left-lateral, transpressional margin in Itanos area (eastern Crete). The cataclastic zone along the fault contact is up to 4 m, in width. (b) Limestones of Tripolitsa nappe are carried along a low-dipping thrust fault above Middle Miocene conglomerates (Vrionisi Peninsula-northern part of Ierapetra basin). (c) The transpressional margin in Kefalos Peninsula (western Kos). The fault shows significant right-lateral motion along the fault surface and separates Cretaceous limestones (CRET.) from Middle Miocene marine marls (MIOC.). (d) Small scale oblique reverse faults affecting Middle Miocene marls near the thrust contact of the previous photograph (Kefalos Peninsula).

The stress parameters are determined by using the Tensor program (Delvaux, 1993). The program starts with an approximation of the principal axes of orientation, using an improved version of the right dihedral method (see Angelier, 1994, and references therein) and proceeds with a search for the best-fitting tensor. The method is based on the minimization of angular differences between calculated and observed striae along microfaults. Palaeostress analysis using fault-slip data requires, assuming a homogenous stress field, parallelism between shear and slip vectors on a fault plane and independence between faults (Etchecopar et al., 1981; Reches, 1987).

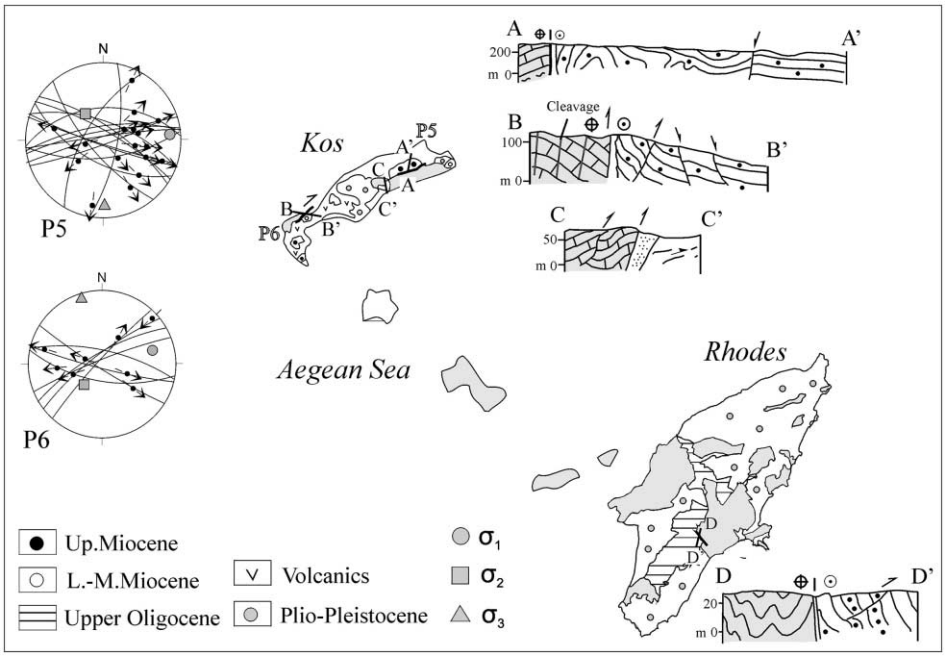

Fig. 6. Simplified map and cross-sections showing contractional structures in Kos and Rhodes Islands. Stereonets outside the map area correspond to subareas with the same letter designation.

The results obtained from the stress analysis are summarized in Table 1. Stress results include the azimuth and the plunge of the three principal stress axes (σ_1, σ_2 and σ_3), which correspond to the principal compressional, intermediate and extensional axes, respectively. The stress ellipsoid shape ratio $R = (\sigma_2 - \sigma_3/\sigma_1 - \sigma_3)$ was also calculated. Parameter [a] defines the average slip deviation between observed and predicted slips on fault planes, for all calculated stress tensors (Table 1). In general, results with average deviation angles less than 30° were considered to be satisfactory. Relative chronology was used for the separation of heterogeneous raw-data fault sets into subsets. Field observations such as consistent fault superposition, syn-sedimentary faults, covered structures and relative age of fault striations guided the assignment of subsets to relative age groups.

4. Stress field and deformation established during the late collisional stage

4.1. Stress field and deformation in Crete

Stress field in Crete is generated during transpression which is characterized by a regional strike-slip stress tensor with subhorizontal σ_1 trending in a NNW-SSE direction, vertical σ_2, and a horizontal σ_3 trending in an E–W direction (Fig. 4: nets P_1, P_3 and P_4). The relative magnitude of the principal stress, expressed as the stress ratio R, is constantly around 0.4 (mean 0.37). The σ_1 axis is parallel to the stretching lineation which is formed during the main orogenic phase in the area (Fig. 2).

Table 1
Palaeostress tensors from fault-slip data[a]

Site	EP	Location	n	σ_1	σ_2	σ_3	R	A	SR
Transpressionall event									
P1		Crete	8	168/05	272/80	80/80	0.50	17	Strike-slip
P2		Crete	16	72/29	199/47	342/29	0.40	11.5	Strike-slip
P3		Crete	7	345/04	246/67	77/22	0.14	9.7	Strike-slip/reverse
P4		Crete	14	173/03	282/80	82/09	0.45	9.7	Strike-slip
P5		Kos	17	85/13	323/66	180/20	0.3	18	Strike-slip/reverse
P6		Kos	8	74/33	240/56	340/07	0.5	15.6	Strike-slip
Transtensional event									
Cr0	1	IB	22	292/72	74/14	167/11	0.58	17.4	Normal
Cr1	1	IB	29	150/81	283/06	13/07	0.46	3.4	Normal
Cr2	1	IB	37	54/81	241/09	151/01	0.57	10.9	Normal
Cr3	1	FB	16	76/69	236/20	329/07	0.71	5.7	Normal /Strike-slip
Cr4	2	IB	10	225/23	75/67	313/02	0.77	6.3	Strike-slip/ normal
Cr5	2	IB	9	358/37	197/51	95/09	0.6	4.5	Strike-slip/ normal
Cr6	2	IB	16	326/69	145/25	55/09	0.69	7.4	Normal/Strike-slip
Cr7	2	FB	36	25/78	202/32	87/01	0.1	6.8	Radial tension
Cr8	2	SB	22	72/83	208/05	298/05	0.41	7.4	Normal
Cr9	2	SB	20	27/70	202/20	292/01	0.44	6.8	Normal
Cr10	2	SB	23	173/17	34/68	267/13	0.60	19.8	Strike-slip/normal
Cr11	2	FB(east)	10	342/73	160/35	81/03	0.37	2.3	Normal
Ks1	1	Kasos	9	69/70	314/08	222/18	0.27	26	Normal
Ks2	2	Kasos	12	351/47	175/43	83/02	0.5	7.4	Normal
KAR1	1	S-Karpathos	6	135/74	270/12	2/11	0.72	18.6	Normal/strike-slip
KAR2	2	E-Karpathos	13	23/46	176/40	278/14	0.81	12.7	Normal/strike-slip
KAR3	2	S-Karpathos	6	259/81	23/05	114/08	0.53	17.4	Normal
KAR4	2	W-Karpathos	10	09/38	202/52	104/06	0.6	16.8	strike-slip/Normal
KAR5	2	W-Karpathos	12	219/64	350/18	86/19	0.61	18.6	Normal/strike-slip
KAR6	2	E-Karpathos	6	170/75	05/15	274/4	0.48	15.6	Normal
KAR7	2	E-Karpathos	12	204/37	15/52	112/04	0.52	21	Strike-slip
R0	1	N-Rhodes	15	181/76	82/02	351/14	0.43	4.5	Normal
R1	1	S-Rhodes	18	44/83	266/5	176/5	0.70	19.8	Normal/strike-slip
R2	2	N-Rhodes	22	294/83	180/03	90/06	0.52	18	Normal
R3	2	E-Rhodes	17	30/76	148/7	240/12	0.61	16.2	Normal/strike slip
R4	2	W-Rhodes	13	67/81	202/06	293/06	0.47	22.3	Normal
R5	2	S-Rhodes	20	193/52	337/33	79/18	0.75	19.8	Normal/strike-slip
K1	1	W-Kos	6	194/78	297/03	28/12	0.33	20.4	Normal
K2	1	E-Kos	6	216/31	81/49	321/24	0.5	12.7	Strike-slip
K3	2	Cent.-Kos	10	72/28	289/56	171/17	0.6	10.3	Strike-slip/normal

[a] EP-extensional phase: 1 = phase A, 2 = phase B, n = number of fault data, σ_1, σ_2, σ_3 = azimuth and plunge of principal stress axes, R = stress ratio, a = average slip deviation (°), SR = stress regime, IB = Ierapetra basin, SB = Sitia basin, FB = Fothia basin.

Deformation, south of Ag. Nikolaos as well as to the east of Sitia, is accommodated by a system of WNW–ESE and NNE–SSW trending oblique reverse faults. The first set includes basin forming faults, whereas the second one comprises only intra-basinal faults.

Near the Kritsa village, Tripolitsa limestones are carried above middle Miocene conglomerates by a WNW–ESE trending, moderate-dipping thrust, showing an oblique-slip sense of movement (Fig. 4a, section AA′). Fault rocks along this fault, associated with the similar in trend Kritsa Fault (KF), comprise cataclasites from Tripolitsa flysch and limestone breccias, up to 4 m thick. Slickensides along the KF indicate left-lateral oblique reverse motions towards the south-southwest. Along this fault zone, footwall uplift took place during sedimentation as it is shown by the accumulation of fault-derived breccias (Postma et al., 1993) and the presence of an erosional unconformity at the base of this succession. The unconformity is also confirmed by dip-data analysis of bedding (Lucchitta and Suneson, 1993; Fig. 3b). Further to the south, near Males village, the middle Miocene deposits are deformed by WNW to NW-SE trending right-lateral strike-slip faults (Fig.4, net P_4).

Another area with WNW–ESE trending transpressional faults is in the north-eastern edge of Crete, where a small basin is down-flexed by two faults which border the northern and southern margins of the basin (Fig. 4b, map and section BB'). Oblique striae and splaying patterns of en-echelon mesoscopic faults, as well, as the offsets of individual segments, indicate a left-lateral, for the northern (Fig. 5a) and right-lateral oblique reverse character of movement for the southern marginal fault. Further south, a smaller basin, on the coastline in the Grantes Gulf is formed along a WNW-trending right-lateral oblique reverse fault, which carries Tripolitsa carbonates above upper-middle Miocene conglomerates (Fig. 4b). Fault rocks along this fault comprise cataclasites, up to 7 m thick, and limestone breccias (Fig. 4, section CC'). Strata in the footwall of the fault are slightly rotated, whereas the hangingwall of the fault is internally deformed by mesoscopic reverse faults and a closely spaced cleavage. In a neighbouring region, near Lagada, a small pop-up structure is formed (Fig. 4b, section DD'). Sedimentary characteristics of all these basins, showing a close association of areas with local basement uplift and erosion and areas of rapid subsidence and deposition, is common in strike-slip regimes (Christie-Blick and Biddle, 1985; Sylvester, 1988).

The NNE–SSW trending strike-slip faults occur within the basin near the Sitia fault (Fig. 4, net P_2). Local stress σ_1 trends parallel to the fault surfaces whereas σ_3 is oriented nearly perpendicular to the faults. As shear stress resolved on the fault surfaces is low it seems very probable that these faults represent weak faults sensu Zoback et al. (1987).

The WNW–ESE and NNE–SSW faults trend parallel to an older transpressional system established during the main orogenic phase. This old fault system caused deviations of the stretching lineation from a regional NNW–SSE trend, providing evidence of strain partitioning during ductile flow (Fig. 2; Kokkalas and Doutsos, 2000). For example, in the Elounda window, this lineation rotates gradually from NNW in the north to WNW in the southern margin of the window, toward the Ag. Nikolaos fault (Fig. 2). A similar distribution of the stretching lineation is also seen in the northern margin of the Selena window area (Fig. 2). This area with oblique kinematics is separated by the Ierapetra fault (IFZ) from an area to the east with orthogonal kinematics (Fig. 2, Ornon window). Also the IFZ provided evidence of strain partitioning during ductile flow.

4.2. Stress field in Kos and Rhodes Islands

The computed stress tensor for the fault population in Kos Island is characterised by a strike-slip stress regime with a sub-horizontal σ_1 trending ENE–WSW, a vertical σ_2 axis and σ_3 trending in a NNW–SSE direction (Fig. 6, nets P5, P6). Deformation is accommodated by ENE–WSW and ESE–WNW trending oblique reverse faults. As σ_3 is perpendicular to the ENE–WSW trending fault surfaces, these faults represent weak faults. Like in the eastern Crete nappe over-thrusting is in a NNW–SSE direction.

In western Kos an ENE-trending fault, separating basement from middle Miocene marine marls, shows a right-lateral oblique reverse slip (Fig. 5c). The fault produced in its footwall a 20 m wide zone internally deformed by oblique thrusts (Fig. 5d) and mesoscopic folds (Fig. 6, section BB′). To the east, an ENE trending right-lateral strike-slip fault is associated with small-scale flexures in Miocene marls (Fig. 6, section AA″). Folds are kink-like in shape, open and verge mainly north-eastwards. Towards the north-east, folds become wider-spaced and beds become gradually horizontal, suggesting decrease of the deformation toward this direction. In the central part of the island, Mesozoic limestones are emplaced tectonically along an oblique thrust, above a monzonitic intrusion, dated as ~12 Ma (Fig. 6, section CC′ Altherr et al., 1982; Henjes-Kunst et al., 1988). The overridden limestones do not show any sign of contact metamorphism even in the immediate vicinity of the intrusion, implying that they were in contact after the uplift and erosion of the monzonite. In the footwall of this fault, the monzonite is internally deformed by S-C structures and low-angle north-dipping shear surfaces, both indicating a top-to-the south-south-east sense of shear.

Limited evidence for contractional deformation comes from Rhodes. In the southern part of the island a WNW–ESE trending, right-lateral strike-slip fault separates upper Oligocene conglomerates from basement units. The flysch is intensively folded, while the sediments are highly rotated near the fault contact and are deformed by low angle thrusts (Fig. 6, section DD′).

5. Stress field and deformation during the fore-arc evolution

The tectonostratigraphy and our fault-slip data analysis in Crete and Dodecanece Islands lead us to distinguish between two phases acting variably during the Upper Miocene and Plio-Pleistocene (Fig. 7).

5.1. Phase A (Late Miocene)

We distinguish between regional and local stress field:

1. Regional stress field is characterised NNW–SSE tension (Fig. 7, stereonets Cr_0, Cr_2, Cr_3, K_2, R_0, R_1 and Fig. 8a). The maximum stress axis (σ_1) was generally vertical, while σ_2 and σ_3 axes were almost horizontal. The σ_3 axis is nearly perpendicular to the axis of tectonic windows formed during the main orogenic phase as well as to the direction of the Hellenic Trench in the area. It corresponds to the σ_3 direction given by Mercier et al. (1987) and Fassoulas (2001).

Extension is accomplished by ENE–WSW trending normal and oblique normal faults. Faults of this set often delimit basement highs from the basin infill, such as the Agios Ioannis Fault

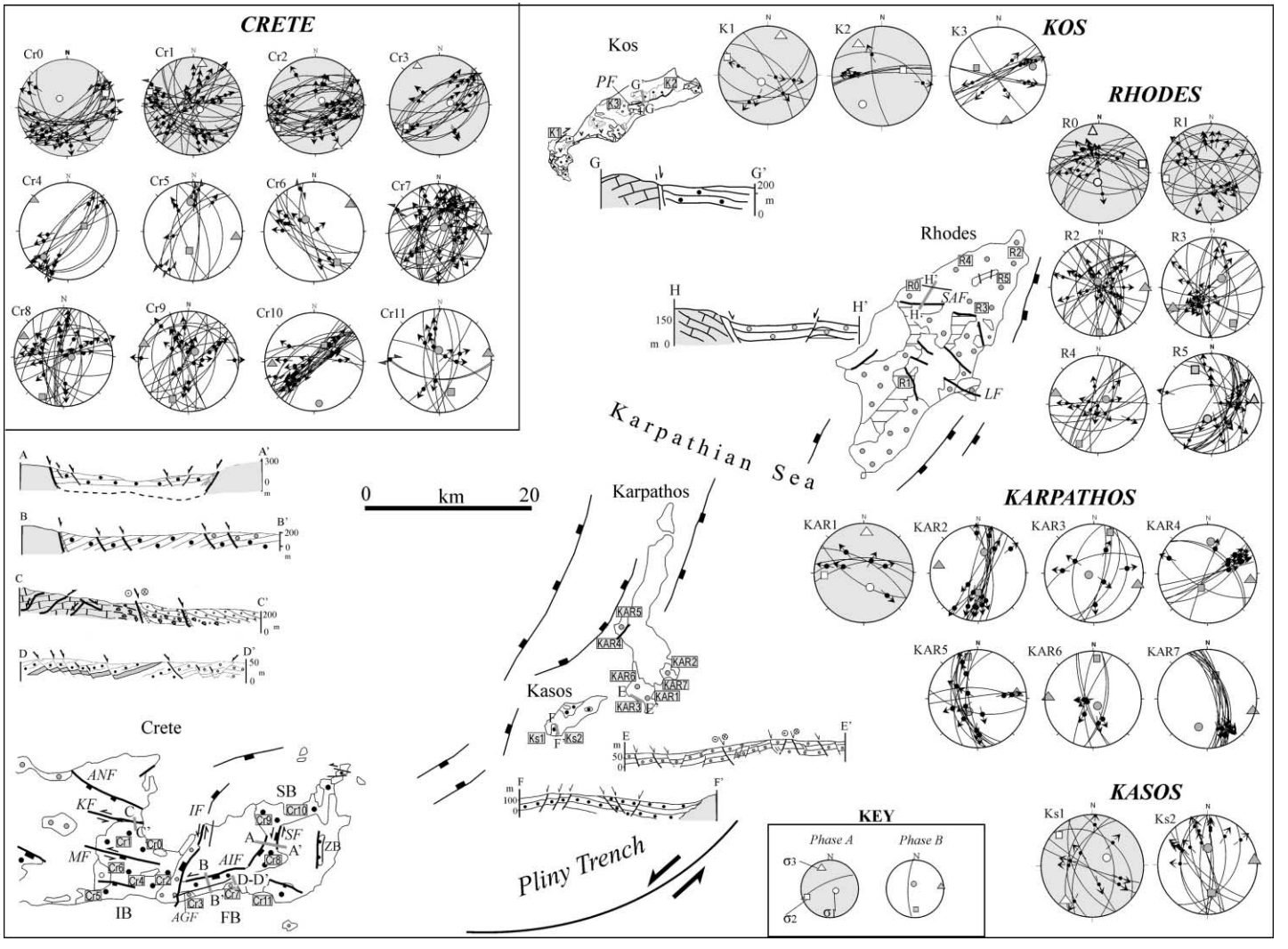

Fig. 7. Neogene structural framework of the SE-Aegean area, showing the variation of stress field from Tortonian to Plio-Pleistocene times. Stereonets outside the map area correspond to subareas with the same letter designation. Stereonets with grey coloring correspond to phase A, white coloring to phase B. Site numbers refer also to Table 1. Symbols on map as in Fig. 4.

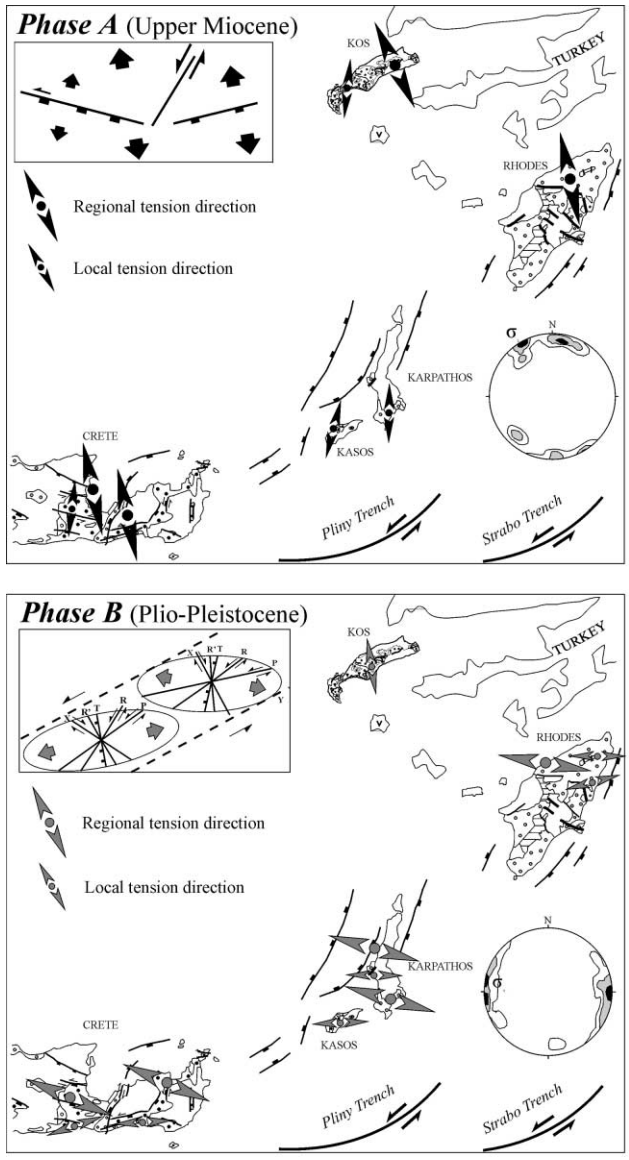

Fig. 8. Regional and local stress fields during the forearc evolution.

(AIF, Fig. 7) in Crete. A series of north-tilted fault-blocks is associated with this fault (Fig. 7: BB′). Some of the ENE–WSW trending faults show a syn-sedimentary origin, as evidenced by the observed rapid changes of sedimentary facies and the frequent presence of wedge-shaped prisms in their hangingwalls (Fig. 7: DD′). Further north on Kos Island, the ENE-WSW trending, steeply-dipping Pili Fault (PL) shows oblique-normal movements (Fig. 7: GG′, net K2).

2. Local stress field is characterized by a NNE-SSW tension (Fig. 7, nets Cr_1, K_1, KAR_1, Ks_1). Extension took place along WNW-ESE oblique normal faults whereas NNE–SSW oblique normal faults played the role of transfer faults. In Crete these faults controlled late Miocene sub-

sidence and sedimentation in the area west of the Ierapetra fault. That is the area where pre-existent, WNW–ESE trending brittle and ductile strike-slip faults, developed during the orogeny of the Hellenides. On a smaller scale this is the case also in the other islands (Fig. 7, nets K_1, KAR_1, Ks_1).

5.2. Phase B (Plio-Pleistocene)

The second phase comprises transtentional to tensional stress tensors with the least principal axis (σ_3) trending variably. The wide divergence of R values indicates that many stations portray transitions from strike-slip to normal solutions (Fig. 7 and Table 1, nets Cr_4, Cr_5, Cr_7, Cr_{10}, Cr_{11}, KAR_2, KAR_4, KAR_5, KAR_6, R_3 and Fig. 8b). Permutations between σ_1 and σ_2 are permitted because their values, relative to σ_3 in many cases, are close in magnitudes (see also Anglelier 1994). Therefore, strike-slip and dip-slip movements represent stress oscillations in time and space rather than discrete stress fields. We distinguish again between regional and local stress field.

1. Regional stress field is characterized by WNW-ESE tension (Fig. 7: Cr_4, Cr_5, Cr_8, Cr_9, R_4, KAR_2, KAR_3, KAR_4, KAR_6, KAR_7) and is oriented perpendicular to NNE–SSW trending faults. In many cases these faults represent reactivations of pre-existed faults, such as the Ierapetra fault in eastern Crete. This fault crosses the island and comprises several similar trending fault strands. The fault trace has a considerable offshore prolongation in both directions, thus forming one of the largest transverse faults of the southern Aegean arc (Mascle and Martin, 1990). The movement inferred from fault kinematics suggests that the IFZ is a normal fault with a sinistral component of motion. Maximum vertical displacements along this fault may exceed 1.5 km (Fytrolakis, 1980). Faulting along this zone and similarly trending faults that transect the western part of Ornon Mountains seem to occur until present, as is indicated by Quaternary fan breccias juxtaposed against the fault scarps, as well as, other morphostructural criteria (Bonnefont, 1977).

Further to the east, two NNE-trending faults controlled the subsidence of two asymmetric basins, the Sitia basin to the west (Fig. 7, section AA′) and the Zakros basin to the east. Borehole data show that the sedimentary infill of the Sitia basin reaches a thickness of $\sim$400 m, being maximum toward the eastern basin margin. Fault kinematic data demonstrate that along the eastern basin-bounding Sitia fault (SF), left-lateral oblique normal movements occurred. A thin ($\sim$100 m) sedimentary cover in the Zakros basin suggests that displacement rates along the Zakros fault (ZF) are minor. Furthermore, offshore studies from the area east of Rhodes and Karpathos confirmed the presence of NNE-striking lineaments, which are interpreted as faults delimiting horst-like structures (Mascle et al., 1986).

In many cases, NNE-trending faults are associated with NNW–SSE trending strike-slip faults (Cr_5, Cr_8, Cr_9, R_5), which do not follow any older fault direction. In other cases NNE-trending faults are scarce and deformation is taken up by ENE–WSW strike slip and oblique normal faults (Fig. 7: Cr_{10}, KAR_4, K_3). These faults display left-lateral oblique normal and strike-slip movements, transecting upper Tortonian sediments in Crete and Plio-Pleistocene sediments in Karpathos (Fig. 7, section EE') and Kos. In western Karpathos island, Upper Pliocene sediments (Buttner and Kowalczyk, 1978) are faulted against an ENE-trending left-lateral strike-slip fault, which strikes parallel to a large offshore fault mapped by Martin and Mascle (1989). Further south in the Kastelo Peninsula Tyrrhenian marine terraces (Barrier et al., 1979; Keraudren and

Sorel, 1984) are cross-cut by oblique normal faults, which are consistent with an E-W orientation of σ_3 (Fig. 7: net KAR_3, section EE′). This east-northeast fault trend is subparallel to the active sinistral transform system, coinciding with structurally controlled troughs such as the Pliny and Strabo trenches (Jongsma, 1977; Le Pichon and Angelier, 1979).

2. Local stress field is characterized by WSW–ENE tension (Fig. 7: Cr_6, Cr_7, Cr_{11}, R_3, R_5, KAR_5, Ks_2). This fault set comprises small intrabasinal faults along which normal and oblique normal movements are taking place. These faults are also confirmed by earthquake focal mechanism solutions, at intermediate depth (Richter and Strobach, 1978).

6. Synthesis and geodynamic implications

Late orogenic basins were originated in association with a transpressional strike-slip stress regime consistent with the regional compression in a NNW–SSE direction, trending parallel to the nappe transport in the area. Deformation took place along pre-existed WNW–ESE and NNE–SSW trending faults formed during ductile transpression in the main orogenic phase. Often during this stage of deformation, NNE–SSW trending faults behave as weak faults caused by a local stress field with the σ_1 trending in a NNE to NE direction. As the eastern Crete has undergone relatively homogenous counter-clockwise rotation of about 30° since the lower Pliocene (Duermeijer et al., 2000) these faults as well as palaeostress axes for this phase must be back rotated accordingly. After this correction regional stress σ_1 becomes nearly N-S and thus deviates strongly from the NE–SW trending 'far field stress' associated with the Africa motion with respect to Europe (Dewey et al., 1989; Fig. 9a). Similarly NNE–SSW trending faults become NE–SW and are parallel to the NE–SW directed transform faults which Robertson et al. (1996) thought to be associated with the opening of the southern Neotethyan strand (inset in Fig. 9). The unconformity, which is confined to the Middle Miocene–Upper Miocene boundary (Fig. 3b) marks the cessation of contractional movements and the progressive establishment of a transtentional stress regime, subdivided in two phases.

Regional stress σ_3 during the first phase in the Upper Miocene is oriented perpendicular to the Pliny and Strabo Trenches as well as to the axes of the tectonic windows suggesting that a mechanism involving arc-normal pull and post-orogenic collapse was responsible for the fore-arc evolution during this time (Figs. 8a and 9b). However, the WNW- and NNE-trending faults, inherited from the previous orogenic phases, were at this time reactivated and caused local stress and deformation.

During the extensional phase in the Plio-Pleistocene time, σ_3 stress varies considerably between the WNW and SW direction. As NNE–SSW trending faults play the most important role in the deformation, WNW–ESE σ_3 direction may represent the regional stress. The fault population consisting of NNE–SSW, NNW–SSE and ENE–WSW oblique normal faults fit well in a theoretical incremental strain pattern of associated secondary strike-slip faults (P and Riedel shears) and pull apart extensional structures predicted by left-lateral simple shear along large scale ENE–WSW trending faults, such as the Pliny and Strabo trenches (Figs. 8b and 9c). The local stress σ_3 in the WSW–ENE direction and associated NNW–SSE trending pull apart structures may be generated during a stronger rotation of the incremental strain as shear stress acting along the trenches progressively increased.

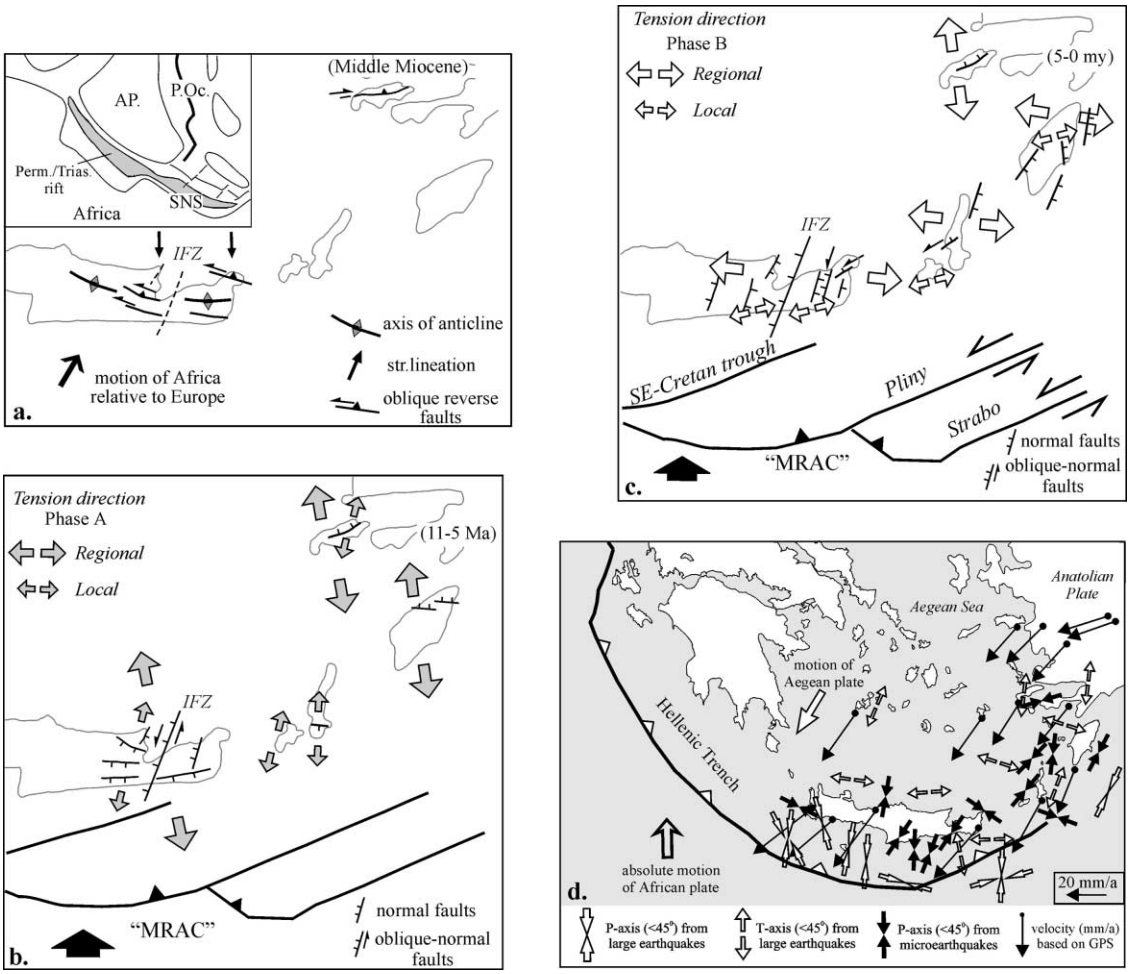

Fig. 9. (a), b) and c) Schematic evolutionary model for the SE-Hellenides. In each stage active structures are indicated. Inset in (a) shows a palaeogeographic reconstruction of the eastern Mediterranean in the Early Jurassic (modified from Robertson et al., 1991). AP = Apulian, P.Oc. = Pindos ocean, SNS = South Neotethyan strand. (d) Combined velocity field (thin black arrows) in the S-SE Hellenic Arc, relative to a Europe-fixed reference frame, based on GPS results (modified from Kahle et al., 1998). Map of P-axes (convergent double arrows) and T-axes (divergent double arrows) that dip shallower than 45°. White double arrows are for large earthquakes, black double arrows are for micro-earthquakes (modified from Hatzfeld, 1999).

An open question is to relate the great variability of intraplate stress and deformation of this phase either with the SSW absolute motion of the Aegean plate or with the N–S absolute motion of the African plate (Fig. 9d). The observed extension across the NNE–SSW trending grabens is compatible with the small extension rates (9 ± 6) registered by GPS measurements in the ESE direction (Robbins et al., 1994; Hatzfeld et al., 1997). However, it is important to note that the maximum motion of the Aegean plate (at 3.5 cm/year) in a SSW direction is not accommodated by any transversely orientated graben structure. This can be explained by a rigid block motion of the Aegean plate without internal deformation as it is pushed westward by the Anatolian plate

(Meijer and Wortel, 1997; Ten Veen and Meijer, 1998). Another possibility is that the NNE–SSW trending faults in the area may act as transfer faults which transmitted movements of the Anatolian plate toward the free edges of the Aegean plate. A similar tectonic pattern is already described in the central Aegean region (Doutsos and Kokkalas, 2001) and in the western Anatolia (Westaway, 1994).

7. Conclusions

1. Stress directions established during the late orogenic phases as well as during the fore-arc evolution in the south-eastern Aegean region are not parallel to the movements of the converging plates in the area.
2. Throughout the tectonic evolution of the area a pre-existing system of WNW–ESE and NNE–SSW trending faults caused a local stress distribution. Shear stress imposed along the south-eastern margin of the Aegean plate during the Plio-Pleistocene caused a great variability of stress as well as a complex pattern of associated structures.
3. The NNE–SSW trending faults may represent reactivation of older transcurrent faults associated with the opening of the Neotethyan ocean. In the present time, they transfer the Anatolian plate motion southwestwards to the Hellenic Trench.
4. We recognize that the pre-existing NNE–SSW trending fault set represents an independent parameter, which controlled local stress evolution in the area and modified plate motions.

Acknowledgements

We thank editing assistance of Professor N. Rast, and incisive reviews by Professor K.D. O'Hara and an anonymous reviewer that improved the paper. SK would like to thank Dr. D. Delvaux for providing the Tensor program for the palaeostress analysis. S.K was financially supported by the Tect/1995 program of the National Grants Foundation of Greece (I.K.Y.).

References

Altherr, R., Kreuzer, H., Wendt, I., Lenz, H., Wagner, G.A., Keller, J., Harre, W., Hohndorf, A., 1982. A late Oligocene/early Miocene high temperature belt in the Attic-Cycladic crystalline complex (SE Pelagonian, Greece). N. Jahrb. Geol. E23 97–164.

Andeweg, B., De Vicente, G., Cloething, S., Giner, J., Munoz Martin, A., 1999. Local stress fields and intraplate deformation of Iberia: variations in spatial and temporal interplay of regional stress sources. Tectonophysics 305, 153–164.

Angelier, J., 1994. Fault slip analysis and palaestress reconstruction. In: Hancock, P. (Ed.), Continental Deformation. Pergamon, Oxford, pp. 53–100.

Angelier, J., Gigout, M., 1974. Sur les plates-formes marines et neotectonique quaternaries de la region de l'Ierapetra (Crete, Grece). C. R. Acad. Sci. Paris 278, 2103–2106.

Angelier, J., Lyberis, N., Le Pichon, X., Barrier, E., Huchon, P., 1982. The tectonic development of the Hellenic arc and the Sea of Crete: a synthesis. Tectonophysics 86, 159–196.

Aubouin, J., Bonneau, M., Davidson, J., Leboulenger, P., Matesco, S., Zambetakis, A., 1976. Esquisse structurale de l'arc egeen externe: des Dinarides aux Taurides. Bull. Soc. Geol. Fr 7, 327–336.

Barrier, E., Angelier, J., 1982. Structure et neotectonique de l'arc hellenique oriental: les iles de Kassos et Karpathos (Dodecanese, Grece). Rev. Geol. Dyn. Geogr. Phys 23, 257–276.

Barrier, E., Muller, C., Angelier, J., 1979. Sur l'importance du Quaternaire ancien marin dans l'ile de Karpathos (Arc Egeen, Grece) et ses implications tectoniques. C. R. Som. Soc. Geol. France 5, 198–201.

Bellon, H., Jarrige, J.J., 1979. L' activite magmatique neogene et quaternaire dans l'ile de Kos, Greece: Donnees radio chronologiques. C. R. Acad. Sci. Paris 288 (Serie D) 1359–1362.

Bernoulli, D., Laubscher, H., 1972. The palinspastic problem of the Hellenides. Eclogae. Geol. Helv 65, 107–118.

Besenecker, H., Otte, O., 1978. Late Cenozoic development of Kos, Aegean Sea. In: Closs, H. et al. (Eds.), Alps, Apennines, Hellenides, pp. 506–509.

Billiris, H., 1991. Geodetic determination of tectonic deformation in Central Greece from 1900 to 1988. Nature 350, 124–129.

Blondeau, A., Fleury, J.J., Guernet, C., 1975. Sur l' existence, dans l' ile de Kos (Dodecanese, Grece), d' une serie neritique surmontee d'un flysch d' age Cuisien superieur on Lutetien inferieur a sa base. C. R. Acad. Sci. Paris 280, 817–819.

Boger, H., Gersonde, R., Willmann, R., 1974. Das Neogen im Osten der Insel Kos (Agais, Dodekanes)-Stratigraphie und Tektonik. N. Jb. Geol. Palaont. Abh 145, 129–152.

Bonnefont, J.C., 1977. La neotectonique et sa traduction dans le paysage geomorphologique de l'Ile de Crete (Grece). Rev. Geogr. Phys. Geol. Dyn 14, 93–108.

Boronkay, K., Doutsos, T., 1994. Transpression and transtension within different structural levels in the central Aegean region. J. Struct. Geol 16, 1555–1573.

Buttner, D., Kowalczyk, G., 1978. Late Cenozoic Stratigraphy and Paleogeography of Greece- a review. In: Closs, H., Roeder, D., Schmidt, K. (Eds.), Alps, Appenines, Hellenides. Verlagbuchandlung, Stuttgart, pp. 494–501.

Christie-Blick, N., Biddle, K.T., 1985. Deformation and basin formation along strike-slip faults. In: Biddle, K.T., Christie-Blick, N., (Eds.), Strike-slip Deformation, Basin Formation and sedimentation. Soc. Econ. Paleont. Miner. Spec. Publ. 37, pp. 1–34.

Creutzburg, N., Seidel, E., 1975. Zum Stand der Geologie des Praneogens auf Kreta. N. Jb. Geol. Palaontol. Abh 149, 363–383.

Delvaux, D., 1993. The TENSOR program for reconstruction: examples from the east African and the Baikal Rift Systems. Terra Abstr., Abstr. Suppl. Terra Nova 5, 216.

Dermitzakis, M.D., Triantaphyllou, M.V., 1991. Contribution to the stratigraphy of Miocene sediments of Kassos island (South Sporades). Bull. Geol. Soc. Greece XXV/ 2, 529–548.

Dewey, J.F., Helman, M.L., Turco, E., Hutton, D.H.W., Knott, S.D., 1989. Kinematics of the Western Mediterranean. In: Coward, M.P., Dietrich, D., Park, R.G. (Eds.), Alpine Tectonics. Spec. Publ. Geol. Soc, London, pp. 265–283.

Dewey, J.F., Pitman, W.C., Ryan, W.B.F., Bonnin, J., 1973. Plate tectonics and the evolution of the Alpine system. Bull. Geol. Soc. Am. 84, 3137–3180.

Dewey, J.F., Sengor, A.M.C., 1979. Aegean and surrounding regions: Complex multiplate and continuum tectonics in a convergent zone. Bull. Geol. Soc. Am. 90, 84–92.

Doutsos, T., Kokkalas, S., 2001. Stress and deformation patterns in the Aegean region. Journal of Structural Geology 23 / 2- 3, 455–472.

Doutsos, T., Koukouvelas, I., Poulimenos, G., Kokkalas, S., Xypolias, P., Skourlis, K., 2000. An exhumation model of the south Peloponnesus, Greece. Int. J. Earth Sci. 89, 350–365.

Drooger, C.W., Meulenkamp, J.E., 1973. Stratigraphic contributions to the geodynamics in the Mediterranean area: Crete as a case history. Bull. Geol. Soc. Greece 10, 193–200.

Duermeijer, C.E., Nyst, M., Meijer, P.Th, Langereis, C.G., Spakman, W., 2000. Neogene evolution of the Aegean arc: paleomagnetic and geodetic evidence for a rapid and young rotation phase. Earth Planetary Science Letters 176, 509–525.

Etchecopar, V., Vasseur, G., Daignieres, M., 1981. An inverse problem in microtectonics for the determination of stress tensors from fault striation analysis. J. Struct. Geol 3, 51–65.

Fassoulas, C., 2001. The tectonic development of a Neogene basin at the leading edge of the active European margin: the Heraklion basin, Crete, Greece. Journal of Geodynamics 31, 49–70.

Fassoulas, C., Kilias, A., Mountrakis, D., 1994. Postnappe stacking extension and exhumation of high-pressure/low-temperature rocks in the island of Crete, Greece. Tectonics 13, 127–138.

Fortuin, A.R., 1977. Stratigraphy and sedimentary history of the Neogene deposits in the Ierapetra region, eastern Crete. GUA Pap. Geol. Series 1, 8. pp 164.
Fortuin, A.R., 1978. Late Cenozoic history of eastern Crete and implications for the geology and geodynamics of the southern Aegean area. Geol. Mijnb 57, 451–464.
Fytrolakis, N., 1980. Der geologische Bau von Kreta. Probleme, Beobachtungen und Erbebnisse. Habil thesis, Technical University of Athens, pp 146.
Hancock, P.L., 1985. Brittle microtectonics: principles and practice. J. Struct. Geol. 7, 437–457.
Hanken, N.-M., Bromley, R., Miller, J., 1996. Plio-Pleistocene sedimentation in coastal grabens, north-east Rhodes, Greece. Geol. J. 31, 393–418.
Hatzfeld, D., 1999. Tectonics and seismicity in the Aegean. In: Durand, B., Jolivet, L., Horvath, F., Seranne, M. (Eds.), The Mediterranean Basins: Tertiary extension within the Alpine Orogon. Geol. Soc. Spec. Publ. 156, 415–426.
Hatzfeld, D., Martinod, J., Bastet, G., Gautier, P., 1997. An analog experiment for the Aegean to describe the contribution of gravitational potential energy. J. Geophys. Res. 102, 649–659.
Henjes-Kunst, F., Altherr, R., Kreuzer, H., Hansen, B.T., 1988. Disturbed U-Th-Pb systematics of young zircons and uranothorites: the case of the Miocene Aegean granitoids (Greece). Chem. Geol 73, 125–145.
Hillis, R.R., Reynolds, S.D., 2000. The Australian Stress Map. Journal of the Geological Society, London 157, 915–921.
Huchon, P., Lyberis, N., Angelier, J., Le Pichon, X., Renard, V., 1982. Tectonics of the Hellenic trench: a synthesis of sea-beam and submersible observations. Tectonophysics 86, 69–112.
Jackson, J.A., 1994. Active tectonics of the Aegean region. Annual Review Earth and Planetary Science 22, 239–271.
Jackson, J.A., King, G., Vita-Finzi, C., 1982. The neotectonics of Aegean: an alternative view. Earth and Planetary Science Letters 61, 303–318.
Jacobshagen, V., Durr, S., Kockel, F., Kopp, K.O., Kowalczyk, G., 1978. Structure and geodynamic evolution of the Aegean region. In: Closs, H., Roeder, D., Schmidt, K. (Eds.), Alps, Apennines, Hellenides. Int. Union Comm. Geodyn. Sci. Rep. 38, 537–564.
Jongsma, D., 1977. Pliny and Strabo Trenches, south of the Hellenic Arc. Bull. Geol. Soc. Am 88, 797–805.
Kahle, H.G., Straub, C., Reilinger, R., McClusky, S., King, R., Hurst, K., Kastens, K., Cross, P., 1998. The strain rate field in the eastern Mediterranean region, estimated by repeated GPS measurements. Tectonophysics 294, 237–252.
Keller, J., Rehren, T.H., Stadlbauer, E., 1990. Explosive volcanism in the Hellenic Arc: a summary and review. In: Hardy, D.A., Keller, J., Galanopoulos, V.P., Flemming, N.C., Druitt, T.H. (Eds.), Thera and the Aegean world III, 2, Earth Sciences. Proc. Third Int. Congress Santorini, Greece, pp. 13-26.
Keraudren, B., Sorel, D., 1984. Relations entre sedimentation, tectonique et morphologie dans le Plio-Pleistocene de Karpathos (Grece); mouvements verticaux et datations radiometriques. L'Anthropologie 88, 49–61.
Kissel, C., Laj, C., 1988. The Tertiary geodynamical evolution of the Aegean arc: a palaeomagnetic reconstruction. Tectonophysics 146, 183–201.
Kokkalas, S., Doutsos, T., 2000. Strain partitioning along the south Hellenides (Eastern Crete, Greece). In: Panayides, I., Xenophontos, C., and Malpas, J. (Eds.), Proceedings of the Third International Conference on the Geology of the Eastern Mediterranean. Geol. Surv. Dept., Cyprus, 83-95.
Le Pichon, X., Angelier, J., 1979. The Hellenic Arc and Trench system: a key to the Neotectonic evolution of the eastern Mediterranean area. Tectonophysics 60, 1–42.
Le Pichon, X., Chamot-Rooke, N., Lallemant, S., Noomen, R., Veis, G., 1995. Geodetic determination of the kinematics of central Greece with respect to Europe: Implications for eastern Mediterranean tectonics. J. Geophys. Res. 100, 12675–12690.
Lucchitta, I., Suneson, N.H., 1993. Dips and extension. Geol. Soc. Am. Bull. 105, 1346–1356.
Martin, L., Mascle, J., 1989. Structure et evolution recente de la mer Egee: II. Le domaine egeen central.. C. R. Acad. Sci. Paris 309, 1487–1493.
Mascle, J., Martin, L., 1990. Shallow structure and recent evolution of the Aegean Sea: A synthesis based on continuous reflection profiles. Mar. Geol. 94, 271–299.
Mascle, J., Le Cleach, A., Jongsma, D., 1986. The Eastern Hellenic margin from Crete to Rhodes: example of progressive collision. Marine Geology 73, 145–168.
Mattauer, M., Mercier, J.L., 1980. Microtectonique et grande tectonique. Mem. H. ser. Soc. Geol. France 10, 133–153.
McKenzie, D., 1972. Active tectonics of the Mediterranean region. Geophys. J. R. Astron. Soc. 30, 109–182.

McKenzie, D., 1978. Active tectonics of the Alpine-Himalayan belt: the Aegean Sea and surrounding regions. Geophys. J. R. Astron. Soc. 55, 217–254.
Meijer, P.T., Wortel, M.J.R., 1997. Present-day dynamics of the Aegean region: a model analysis of the horizontal pattern of stress and deformation. Tectonics 16, 879–895.
Mercier, J.L., Sorel, D., Simeakis, K., 1987. Changes in the state of stress in the overriding plate of a subduction zone: the Aegean Arc from the Pliocene to the present. Ann. Tectonicae 1, 20–39.
Mercier, J.L., Sorel, D., Vergely, P., Simeakis, K., 1989. Extensional tectonic regimes in the Aegean basins during the Cenozoic. Basin Research 2, 49–71.
Meulenkamp, J., De Mulder, F.J., De Weerd, A., 1972. Sedimentary history and Paleogeography of the Late Cenozoic of the island of Rhodos. Z. Deutsch. Geol. Ges. 123, 541–553.
Mutti, E., 1965. Submarine flood tuffs (ignimbrites) associated with turbidites in Oligocene deposits of Rhodes island (Greece). Sedimentology 5, 265–288.
Mutti, E., Orombelli, G., Pozzi, R., 1970. Geological studies of the Dodecanese Islands (Aegean Sea)-Geological map of the Island of Rhodes and explanatory notes. Ann. Geol. Pays. Hell. 22, 77–226.
Petit, J.P., 1987. Criteria for the sense of movement on fault surfaces in brittle rocks. J. Struct. Geol. 9, 597–608.
Pirazzoli, P.A., Thommeret, J., Thommeret, Y., Laborel J., Montaggioni, L.F., 1982. Crustal block movements from Holocene shorelines: Crete and Antikythira (Greece). In: Le Pichon, X., Augustidis, S., Mascle, J. (Eds.), Geodynamics of the Hellenic Arc and Trench. Tectonophysics 86, 27–43.
Postma, G., Fortuin, A.R., Van Wamel, W.A., 1993. Basin-fill patterns controlled by tectonics and climate: the Neogene 'fore-arc' basins of eastern Crete as a case history. Spec. Publ. Int. Ass. Sedim. 20, 335–362.
Rebai, S., Philip, H., Taboada, A., 1992. Modern tectonic stress field in the Mediterranean region: evidence for variation in stress directions at different scales. Geophys. J. Int. 110, 106–140.
Reches, Z., 1987. Determination of the tectonic stress tensor from slip along faults that obey the Coulomb yield condition. Tectonics 6, 849–861.
Richter, I., Strobach, K., 1978. Benioff zones of the Aegean Arc. In: Closs, H., Roeder, D., Schmidt, K. (Eds.), Alps, Apennines, Hellenides. Int. Union Comm. Geodyn. Sci. Rep. Vol. 38, pp. 410–414.
Robbins, J.W., Dunn, P.J., Torrence, H., Smith, D.E., 1994. Deformation in the Eastern Mediterranean. Paper presented at First Turkish Symposium on Deformations, UCTEA-Chamber of Surv. Eng. of Turkey, Instabul, 5–9 September.
Roberts, G.P., 1996. Variation in fault-slip directions along active and segmented normal fault systems. J. Struct. Geol. 18, 835–845.
Robertson, A.H.F., Clift, P.D., Degnan, P., Jones, G., 1991. Palaeogeographic and palaeotectonic evolution of the Eastern Mediterranean Neotethys. Palaeogeogr. Palaeoclimatol. Palaeoecol. 87, 289–344.
Robertson, A.H.F., Dixon, J.E., Brown, S., Collins, A., Morris, A., Pickett, E., Sharp, I., Ustaomer, T., 1996. Alternative tectonic models for the Late Palaeozoic–Early Tertiary development of Tethys in the Eastern Mediterranean region. In: Morris, A., Tarling, D.H. (Eds.), Palaeomagnetism and Tectonics of the Mediterranean Region. Geol. Soc. Spec. Publ., Vol. 105, pp. 239–263.
Sassi, W., Faure, J.-L., 1997. Role of faults and layer interfaces on the spatial variation of stress regimes in basins: inferences from numerical modelling. Tectonophysics 266, 101–119.
Seidel, E., Kreuzer, H., Harre, W., 1982. A late Oligocene/early Miocene high pressure belt in the external Hellenides. Geol. Jahrb 23, 165–206.
Smith, A.G., 1977. Othris, Pindos and Vourinos ophiolites and the Pelagonian zone. Proc. VI Colloq. Geol. Aegean Region (Athens) 3, 1369–1374.
Smith, P.E., York, D., Chen, Y., Evensen, N.M., 1995. The timing of an ancient Greek paroxysm on the island of Kos: towards a more precise calibration of the Mediterranean Deep-Sea Record. American Geophysical Union, December 1995, fall meeting, Abstracts, F 712.
Spang, J.H., 1972. Numerical method for dynamic analysis of calcite twin lamellae. Geol. Soc. Am. Bull. 83, 467–472.
Stockhert, B., Wachmann, M., Schwarz, S., 1995. Structural evolution and rheology of high-pressure-low-temperature metamorphic rocks. Boch. Geol. Geot. Arb. 44, 235–242.
Sylvester, A.G., 1988. Strike-slip faults. Geol. Soc. Am. Bull. 100, 1666–1703.
Ten Veen, J., Meijer, P., 1998. Late Miocene to Recent tectonic evolution of Crete (Greece): geological observations and model analysis. Tectonophysics 298, 191–208.

Ten Veen, J.H., Postma, G., 1999. Neogene tectonics and basin fill patterns in the Hellenic outer-arc (Crete, Greece). Basin Res. 11, 223–241.

Thomson, S.N., Stockhert, B., Rauche, H., Brix, M.R., 1998. Thermochronology of the high-pressure metamorphic rocks of Crete, Greece: implications for the speed of tectonic processes. Geology 26, 259–262.

Tikoff, B., Wojtal, S.F., 1999. Displacement control of geologic structures. Journal of Structural Geology 21, 959–967.

Turner, F.J., 1953. Nature and dynamic interpretation of deformation lamellae in calcite of three marbles. Am. J. Sci. 251, 276–298.

Westaway, R., 1994. Evidence for dynamic coupling of surface processes with isostatic compensation in the lower crust during active extension of western Turkey. J. Geophys. Res. 99, 20203–20223.

Willmann, R., 1983. Neogen und jungtertiare Entwicklung der Insel Kos (Agais, Griechenland). Geol. Rundsch 72, 815–860.

Xypolias, P., Doutsos, T., 2000. Kinematics of rock flow in a crustal-scale shear zone: implication for the orogenic evolution of the southwestern Hellenides. Geol. Mag. 137, 81–96.

Zoback, M.D., 1987. New evidence on the state of stress of the San Andreas fault system. Science 238, 1105–1111.

Zoback, M.L., 1989. State of stress and modern deformation of the Northern Basin and Range Province. J. Geophys. Res. 94, 7105–7128.

Zoback, M.L., 1992. First- and second-order patterns of stress in the lithosphere: the world stress map project. J. Geophys. Res. 97, 11703–11728.